Journal of Hazardous Materials 411 (2021) 125118

Contents lists available at ScienceDirect

Journal of Hazardous Materials

journal homepage: www.elsevier.com/locate/jhazmat

Fungal enzymes for the degradation of polyethylene: Molecular docking simulation and biodegradation pathway proposal

Ericka Santacruz-Juárez [b], Ricardo E. Buendia-Corona [c], Ramsés E. Ramírez [c], Carmen Sánchez [a,*]

[a] Laboratory of Biotechnology, Research Centre for Biological Sciences, Universidad Autónoma de Tlaxcala, Ixtacuixtla, Tlaxcala C.P. 90120, Mexico
[b] Universidad Politécnica de Tlaxcala. San Pedro Xalcatzinco, Tepeyanco, Tlaxcala C. P. 90180, Mexico
[c] Departamento de Fisicomatemáticas, Facultad de Ciencias Químicas, Benemérita Universidad Autónoma de Puebla, Av. San Claudio y 14 Sur, Col. San Manuel, C.P. 72570, Puebla, Pue., Mexico

ARTICLE INFO

Editor: Dr. R. Maria Sonia

Keywords:
Laccase
Molecular docking
Peroxidase
Polyethylene biodegradation
Unspecific peroxygenase

ABSTRACT

Polyethylene (PE) is one of the most highly consumed petroleum-based polymers and its accumulation as waste causes environmental pollution. In this sense, the use of microorganisms and their enzymes represents the most ecofriendly and effective decontamination approach. In this work, molecular docking simulation for catalytic enzyme degradation of PE was carried out using individual enzymes: laccase (Lac), manganese peroxidase (MnP), lignin peroxidase (LiP) and unspecific peroxygenase (UnP). PE-binding energy, PE-binding affinity and dimensions of PE-binding sites in the enzyme cavity were calculated in each case. Four hypothetical PE biodegradation pathways were proposed using individual enzymes, and one pathway was proposed using a synergic enzyme combination. These results show that in nature, enzymes act in a synergic manner, using their specific features to undertake an extraordinarily effective sequential catalytic process for organopollutants degradation. In this process, Lac (oxidase) is crucial to provide hydrogen peroxide to the medium to ensure pollutant breakdown. UnP is a versatile enzyme that offers a promising practical application for the degradation of PE and other pollutants due to its cavity features. This is the first *in silico* report of PE enzymatic degradation, showing the mode of interaction of PE with enzymes as well as the degradation mechanism.

1. Introduction

Plastic products are very useful for society since they bring comfort and convenience at low cost to our daily lives. However, the growing amount of plastic waste is a global concern because it causes environmental pollution. Plastic pollution is spread throughout the world's oceans by prevailing winds and surface currents, with some of it ending up in the digestive system of marine animals, which finally affects human health (Quero and Luna, 2017). It has been estimated that almost 6.4 million tons of waste is introduced into marine environments annually (Agamuthu, 2018). In terms of the global composition of marine litter, plastics account for 62.31%. Plastics also contribute 49% of the litter composition in the seafloor and 81% on the sea surface (Litterbase; https://litterbase.awi.de/). In addition, contamination of soils with small plastic particles causes visual derogation of the landscape and the release of greenhouse gases and hazardous chemicals (de Souza-Machado et al., 2018). It has been reported the negative impact of plastic pollution in soil invertebrates. In particular, polyethylene microplastics had adverse effects on the gut microbial community, reproduction and behaviors of the soil springtail, *Folsomia candida* (Ju et al., 2019; Selonen et al., 2020; Helmberger et al. 2020). Polyethylene (PE) is the most common produced thermoplastic and constitutes the majority of plastic waste within municipal solid waste (Pathak and Navneet, 2017; Sánchez, 2020).

PE is a polymer of ethylene and represents several different polymers having similar chemical structure, but different properties, which arise from subtle differences in molecular architecture. For example, linear PE has high symmetry and it is commonly known as high-density polyethylene (HDPE). Low-density polyethylene (LDPE) contains long and short irregular branches and it is widely used in plastic bags as its low

Abbreviation: PE, Polyethylene; Lac, laccase; MnP, Manganese peroxidase; LiP, Lignin peroxidase; UnP, Unspecific peroxygenase; Cut, Cutinase; PDB, Protein Data Bank; K_{ed}, Dissociation constant.

* Corresponding author.
E-mail address: carmen.sanchezh@uatx.mx (C. Sánchez).

https://doi.org/10.1016/j.jhazmat.2021.125118
Received 14 October 2020; Received in revised form 17 December 2020; Accepted 8 January 2021
Available online 14 January 2021

density makes it light and flexible. HDPE, on the other hand, is harder and offers higher strength and better resistance to heat. HDPE refers to a material with a molecular weight of 100–250,000 Daltons whereas LDPE has a molecular weight of about 40,000 Daltons (Kurtz and Manley, 2009).

It is crucial to develop environmentally friendly tools for decontamination of the environment. In this sense, fungi possess machinery involving unspecific enzymes that catalyze a diversity of reactions, which makes them highly effective for the degradation of environmental pollutants (Sánchez, 2020). Several studies have demonstrated fungal

Table 1
Current research on degradation of polyethylene by fungi.

Organism	Origin of the strain	PE used in the study	Type of study	Findings	Reference
Aspergillus flavus	Guts of wax moth *Galleria mellonella*	HDPE-microplastic particles (HDPE-MPP)	*In vitro*	HDPE-MPP was degraded into MPP with a lower molecular weight after 28 d. Two laccase-like multicopper oxidases genes, displayed up-regulated expression during the biodegradation process.	Zhang et al. (2020)
Cephalosporium sp	National Collection of Industrial Microorganism strain NCIM 1251(Pune, India).	HDPE films (nitric acid-pretreated)	*In vitro*	Gravimetric analysis showed a decrease in weight of HDPE by 7.18% after 20 days of incubation period.	Chaudhary and Vijayakumar (2020)
Aspergillus terreus, Aspergillus sydowii	Rhizosphere soil of *Avicennia marina*	PE	*In vitro*	Fungal strains were efficient in PE degradation after 60 d of growth.	Sangale et al. (2019)
Trichoderma viride, Aspergillus nomius	Landfill soil.	LDPE films	*In vitro*	*T. viride* and *A. nomius* reduced weight of LDPE film after 45 d of growth.	Munir et al. (2018)
Aspergillus oryzae	Dandora dumpsite (Kenya)	LDPE sheets	*In vitro*	LDPE sheets showed a weight reduction after 4 months.	Muhonja et al. (2018)
Rhizopus oryzae	Not reported	LDPE film (thermally treated)	*In vitro*	About 8.4% decrease (gravimetrically) in weight and 60% reduction in tensile strength of PE was observed after 30 d of growth.	Awasthi et al. (2017)
Penicillium oxalicum and Penicillium chrysogenum	Soil sample from a plastic dumping	HDPE and LDPE sheets	*In vitro*	Morphological damages were observed on PE sheets after 60 d of growth.	Ojha et al. (2017)
Zalerion maritimum	American Type Culture Collection strain 34329	PE microplastics	*In vitro*	This marine fungus was able of utilizing PE microplastic, showing the decrease in both, size and mass of the pellets after 28 d (requiring minimum nutrients).	Paço et al. (2017)
Aspergillus niger	Municipal solid waste	LDPE sheets	*In vitro*	*A. niger* had the greatest biodegradation efficiency of LDPE after 90 d culture.	Raghavendra et al. 2016)
Aspergillus niger, Aspergillus flavus	Garbage soil	LDPE granules	*In vitro*	Reduction of 26% (with *A. niger*) and 16% (with *A. flavus*) in molecular weight for a period of 6 months.	Deepika and Jaya (2015)
Aspergillus caespitosus, Phialophora alba, Paecilomyces variotii, Aspergillus terreus, Alternaria alternate, Eupenicillium hirayamae	Mangrove of Red Sea coast	LDPE film	*In vitro*	Strains were able to growth on LDPE. Enzymatic activity (Laccase, MnP and LiP) were detected after 4 weeks. Their consortium had the highest enzymatic activity (MnP showed the greatest activity).	Ameen et al. (2015)
Trichoderma harzianum	Soil sample of dumpsites	PE (autoclaved, UV-treated, and surface-sterilized)	*In vitro*	*T. harzianum* was able to degrade UV-treated PE (40%) more efficiently than autoclaved (23%) and surface-sterilized PE (13%) after 3 months. Enzymes responsible for PE were identified as laccase and manganese peroxidase.	Sowmya et al. (2014)
Fusarium sp., *Penicillium* sp., *Aspergillus niger, Aspergillus japonicus* and *Aspergillus flavus*, *Mucor* sp.	Polyethylene polluted sites	LDPE sheets	*In vitro*	*A. japonicas, Fusarium* sp. and *A. flavus* degraded 36%, 32% and 30%, respectively, the rest of the strains degraded around 20% in terms of weight loss (after 4 weeks).	Singh and Gupta (2014)
Aspergillus sp., *Fusarium* sp.	Soil buried LDPE films	LDPE films	*In vitro*	Decrease in weight of LDPE films was observed over a period of 60 d.	Das and Kumar (2014)
Aspergillus terreus	Plastic waste dump yard	HDPE (UV-pretreated)	*In vitro*	The strain was found efficient in degrading HDPE by weight loss after 30 d.	Balasubramanian et al. (2014)
Aspergillus niger (a mixed culture with *Lysinibacillus xylanilyticus*)	Landfill soils	LDPE films	*In vitro*	The percentages of biodegradation were 29% and 16% for the UV-irradiated and non-UV-irradiated LDPE films, respectively, after 126 d.	Esmaeili et al. (2013)
Mucor hiemalis, Aspergillus versicolor, Aspergillus niger, Aspergillus flavus, Penicillium sp., Chaetomium globosum, Fusarium oxysporum, Fusarium solani, Phoma spp., *Chrysonilia setophila*	Plastic buried in soil	PE (plastic sheets)	*In vitro*	The strain *A. flavus, F. oxysporum* and *Phoma* spp., were able to breakdown efficiently PE after 2 months.	Sakhalkar and Mishra (2013)
Aspergillus versicolor, Aspergillus sp.	Sea water	LDPE film	*In vitro*	LDPE was degraded into CO_2. *A. versicolor* and *Aspergillus* sp evolved around 4 and 3.8 g/l of CO_2, respectively in a week.	Sindujaa et al. (2011)
Aspergillus fumigatus, Aspergillus terreus, Fusarium solani	Aerobic aged municipal landfill	LDPE (25 days under UV-irradiation)	*In vitro*	*A. terreus* and *A. fumigatus* could utilize LDPE as carbon source after 100 d (SEM and FTIR spectroscopy were used).	Zahra et al. (2010)

degradation of PE, however, very little is known about the enzymes involved in the PE degradation process (Table 1). It is recognized that both enzymatic and abiotic factors (e.g., UV light) can mediate the initial oxidation of PE chains, and it has been suggested that the metabolic pathways for degradation of hydrocarbons can be utilized once the size of PE molecules decrease to an adequate dimension for enzyme action (typically from 10 to 50 carbons) (Restrepo-Flórez et al., 2014). In addition, fungi are capable of producing hydrophobins for adhesion of hyphae to plastic surfaces (e.g., PE) (Sánchez, 2020). Hydrophobins are crucial surface proteins for the bioremediation process due to their role as biosurfactants, which improve substrate bioavailability. These proteins can be divided on the basis of their solubility into Class I, which is highly insoluble in aqueous solutions, and Class II, which is soluble in aqueous dilutions of organic solvents (Wu et al. 2017). Several studies have reported fungal capability for PE degradation, in which enzymes such as peroxidases and oxidases have been involved (Ojha et al., 2017; Munir et al., 2018; Muhonja et al., 2018; Sangale et al., 2019; Sánchez et al., 2020). Structurally, enzymes are proteins that contain an active site to which substrate binds and where the chemical reaction catalyzed by the enzyme occurs (Demain and Sánchez, 2017). It has been reported that the use of molecular docking to study ligand enzyme interactions is crucial to understand the enzyme catalytic mechanisms of organopollulants and their application in environmental remediation (Librando and Pappalardo, 2013; Sridhar and Chandra, 2014; Fecker et al., 2018; Liu et al., 2018a, 2018b; do Canto et al., 2019; Li et al., 2019; Srinivasan and Sadasivam, 2018; Srinivasan et al., 2019; Zígolo et al., 2020). Molecular docking is a computational tool that can be used to model the interaction between an enzyme and an organopollutant at the atomic level, which allows us to characterize the behavior of the substrate in the binding site. This process involves prediction of the substrate susceptibility, conformation and position and orientation within the active site, allowing us to assess its binding affinity and energy affinity (Teng et al., 2011; Singh et al., 2017; Liu et al., 2018a, 2018b; Shao et al., 2019; Wang et al., 2020; Mishra et al., 2021).

In the present work, molecular docking simulation for catalytic enzyme degradation of PE was carried out using individual extracellular enzymes: laccase (Lac), manganese peroxidase (MnP), lignin peroxidase (LiP), unspecific peroxygenase (UnP) or cutinase (Cut; as enzyme negative control). The PE-binding energy, PE-binding affinity and dimensions of the PE-binding site in the cavity of the enzyme were calculated for each case. Four hypothetical PE biodegradation pathways were proposed using individual enzymes (Lac, MnP, LiP or UnP), and one pathway was proposed using a synergic enzyme (MnP, Lac, LiP and UnP) combination. This is the first *in silico* report of PE enzymatic degradation, showing the mode of interaction of PE with enzymes as well as the degradation mechanism (Table 1).

2. Materials and methods

2.1. Enzymes used in the study

The 3D structures of the five enzymes used in the molecular docking simulation were obtained from the Protein Data Bank (PDB; https://www.rcsb.org/). These enzymes were MnP from *Phanerochaete chrysosprium* (Sundaramoorthy et al., 2010), UnP from *Agrocybe aegerita* (Piontek et al., 2013), LiP from *Trametes cervine* (Miki et al., 2011), Lac from *Trametes versicolor* (Bertrand et al., 2002) and Cut from *Fusarium solani* (Martinez et al., 1992), with the codes; 3M5Q, 2YOR, 3Q3U, 1KYA and 1CUS, respectively. The first four enzymes are classified in the oxydoreductase group. MnP, LiP and Lac have been reported to be capable of hydrolyzing PE (Ameen et al., 2015). UnP is a monooxygenase that has not been studied for PE biodegradation. On the other hand, Cut belongs to the hydrolase group, which has not been reported to degrade PE. Cut is an esterase that catalyzes the cleavage of ester bonds (Hernández-Sánchez et al., 2019), which are not present in the PE structure. Cut was used as a negative control in molecular docking.

2.2. Molecular modeling

PE (dodecane; $C_{12}H_{26}$) having a molecular weight, area and volume of 170.3 Daltons, 472.4 $Å^2$, and 206.8 $Å^3$, respectively, was used in this study. It has been reported that the enzyme action takes place once the size of PE molecules decrease to an acceptable range (typically from 10 to 50 carbons (Restrepo-Flórez et al., 2014)).

The three-dimensional structure of PE was built with the GaussView 5.0 program and optimized with RHF/STO-3G (Hartree–Fock method), which is a variational wavefunction-based approach, and B3LYP/6–311G (2d,2p). It is a functional and basis set giving the closest agreement with experimental data (Talebian and Talebian, 2014). All components were calculated by the GAUSSIAN 09 program (Frisch et al., 2010). The local minimum value for PE was established, which corresponds to the positive vibrational frequencies of pure polyethylene at room temperature (Talebian and Talebian, 2014).

2.3. Molecular docking simulation

Molecular simulations were carried out using the software AutoGrid 4.2 for grid map generation and AutoDock 4.2 for pose evaluation (Morris et al., 2009). PE ligand was generated as described before (Section 2.2) and set up as a flexible molecule for docking with the Gasteiger partial charges calculation method (Gasteiger and Marsili, 1980), which allows the software to make torsions between rotatable bonds (any single nonring bond, bounded to nonterminal heavy atoms) (Veber et al., 2002), so the ligand can fit the binding site in an approach closer to what occurs in nature. Atom-type torsions and conversion into appropriate input files were prepared for further use in docking. Fungal enzymes retrieved from PDB were ionized at pH 7.4, set up as rigid structures and prepared as ligands for docking; nonpolar hydrogens were merged. The grid center dimensions were 100 grid points in the X, Y and Z coordinates with 0.2 Å spacing for all of the studied enzymes. Blind docking grid boxes were located around the heme group for MnP, UnP and LnP; surrounding the coordinated bonds with the copper ion for Lac; and covering amino acids Ser120, His188 and Asp175 for Cut. The PE ligand was subjected to 100 independent Lamarckian genetic algorithm runs (Morris et al., 1998) of docking search simulations, and the maximum number of energy evaluations was set to 25,000,000. Cavities, docked structure visualization and hydrophobic surfaces were performed on the UCSF Chimera 1.11.2 package (San Francisco, California, USA) (Pettersen et al., 2004). Detection of cavities and measurement of surfaces (area and volume) were carried out on an automated platform, Computed Atlas of Surface Topography of proteins (CASTp) (Tian et al., 2018).

2.4. PE-binding energy and PE-binding affinity calculation

PE-binding energy and PE-binding affinity values were generated by Autodock and were estimated using the Lamarckian genetic algorithm (Morris et al., 1998). The ligand-binding energy corresponds to the energy required to form the enzyme-ligand complex, and the lowest values are considered to be the best binding conformations (Yadav et al., 2017; Aamir et al., 2018). The binding affinity refers to the strength of the binding interaction between the enzyme and its ligand (Kastritis and Bonvin, 2013; Zago et al., 2016).

2.5. Enzyme-catalyzed PE mechanisms of degradation pathway proposal

Two-dimensional structures of the compounds were drawn using ChemDraw Professional 17.1 software (CambridgeSoft Corporation, USA; www.cambridgesoft.com). Five hypothetical pathways for the enzymatic degradation of PE were proposed. Four of them were proposed using individual enzymes (Lac, MnP, LiP or UnP), and one of them was proposed using a synergic association of three enzymes (Lac, MnP and LiP).

3. Results and discussion

3.1. PE-enzyme complex analysis by molecular docking

In the present work, analysis of the individual interactions between MnP, LiP, Lac, UnP or Cut (as a negative control) and the ligand PE was carried out by computational molecular simulations to determine via optimization of molecular geometries and molecular docking the affinity that these fungal enzymes would have for accepting PE within their catalytic sites. Figs. 1–5 show the enzyme cavities previously (a) and after docking simulation (b). The docked structure of the PE-enzyme complex (c) reflects the location where docking simulation took place, showing the surrounding amino acid residues involved in the best PE pose (d).

Table 2 shows that the binding energy scores were −6.09, −6.0, −5.69 and −5.57 Kcal/mol for PE docked to UnP, Lac, LiP and MnP, respectively. These scores showed that the best binding conformations corresponded to the UnP-PE complex (Fig. 1), followed by the Lac-PE complex (Fig. 2), LiP-PE complex (Fig. 3) and MnP-PE complex (Fig. 4). Cut had the least negative (least favorable) enzyme-PE score (−3.07 Kcal/mol) of all enzymes tested. In fact, PE is not bound to the Cut active site (Fig. 5). These results are in accordance with experimental observations (Ameen et al., 2015). Ameen et al. (2015) reported that MnP, LiP and Lac are fungal enzymes involved in PE degradation. Although UnP has not been studied for PE biodegradation, it is a potential degrader of several hazardous pollutants (Karich et al., 2017, Sánchez, 2020). On the other hand, Cut is not able to degrade PE.

The binding energy scores obtained in the present research are similar to those scores reported previously as efficient values for analogous studies on organopollulant degradation by molecular docking simulation (do Canto et al., 2019; Singh et al., 2017). do Canto et al. (2019) reported favorable interactions between polyurethane (PU)-degrading enzymes and PU as ligand, showing binding energy values between −5.5 Kcal/mol and −7.7 Kcal/mol. Furthermore, Singh et al. (2017) reported that a hydrolase capable of degrading phthalates was most efficiently docked to monoethyl phthalate (MEP), showing binding energy scores of −6.31, −5.86, −5.01 and −4.4 Kcal/mol for MEP, mono butyl phthalate, mono hexyl phthalate and mono ethyl hexyl phthalate, respectively.

On the other hand, the binding affinity is the strength of the binding interaction between the enzyme and its ligand. It is usually measured and reported by the dissociation constant (K_{ed}), which is used to evaluate and rank order strengths of bimolecular interactions (Kastritis and Bonvin, 2013; Zago et al., 2016). In this sense, the larger the K_{ed}, the more weakly the enzyme and ligand are attracted to and bind each other. Therefore, a small K_{ed} value shows a great binding affinity of the ligand (e.g., PE) for the enzyme. In this study, the binding affinity was evaluated by molecular docking. PE-binding affinity was 34.34, 40.11, 66.93, 82.16 and 5590 μM for UnP, Lac, LiP, MnP and Cut, respectively (Table 2). PE showed the lowest and highest binding affinity values when it was bound to UnP and Cut, respectively. This shows that PE has a great binding affinity for UnP, whereas PE is weakly attracted to Cut. In fact, PE is not bound to the Cut catalytic cavity (Fig. 5). These results illustrate the strength of the binding interaction of PE to the enzyme in the following manner: UnP > Lac > LiP > MnP > Cut.

As shown in Table 2, the greatest area (659.920 Å^2) and volume (367.243 Å^3) of the enzyme catalytic cavity (pocket) were exhibited by UnP followed by LiP, MnP, Lac and Cut. UnP showed the largest enzyme cavity, whereas Cut had the smallest enzyme cavity. These results show that UnP had the most ligandable cavity due to its large volume, high area and high hydrophobicity, which are features of a more ligandable pocket (Volkamer et al., 2010, 2012; Isvoran, 2015). UnP had several phenylalanine residues (hydrophobic amino acids) in its cavity, which would facilitate PE binding to the active site where catalysis occurs. Previous studies on molecular docking analysis for PU degradation using polyurethanases (known to degrade PU) showed that monomers of PU had favorable interactions with the modeled enzymes (polyurethanases), showing a cavity area between 512.15 and 2553.82 Å^2

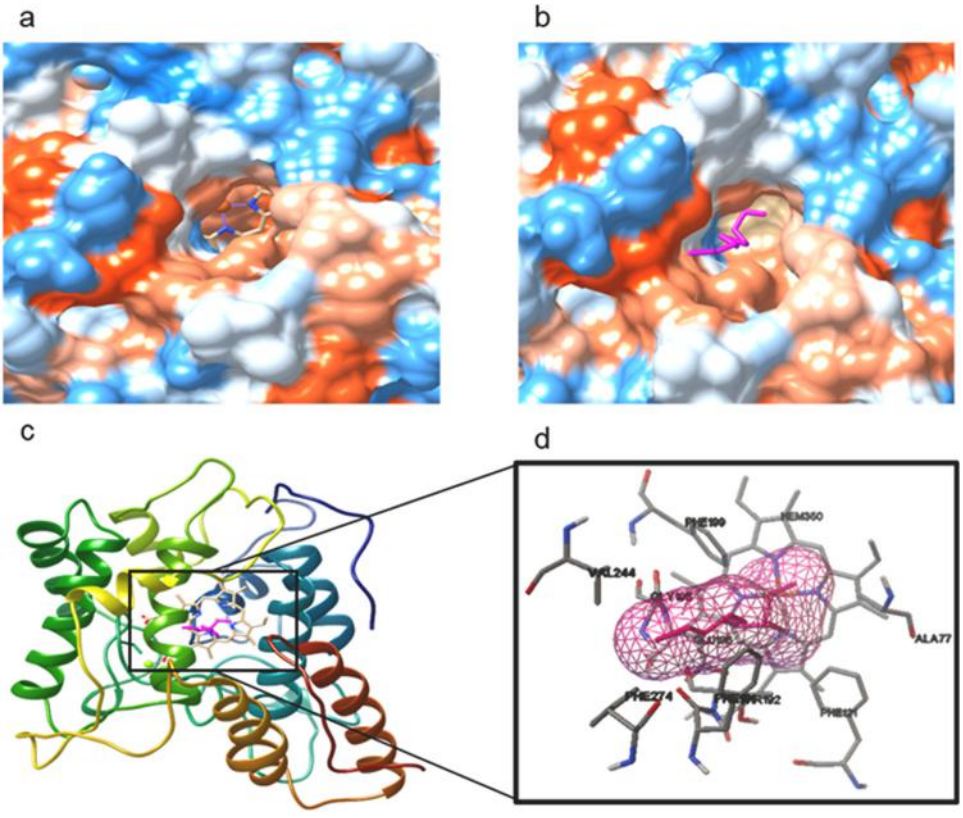

Fig. 1. *In silico* molecular docking analysis of the binding capacity of PE with UnP. UnP cavity (a), representation of the PE-UnP complex hydrophobic surface, PE on magenta (software UCSF Chimera) (b), docked PE-UnP structure, PE on magenta and UnP depicted on secondary structure with rainbow colors from n-terminus in blue to c-terminus in red (software UCSF Chimera) (c), and binding site showing PE in magenta and surrounding amino acid residues on colors by heteroatom (software AutodockTools) (d).(For interpretation of the references to colour in this figure legend, the reader is referred to the web version of this article.)

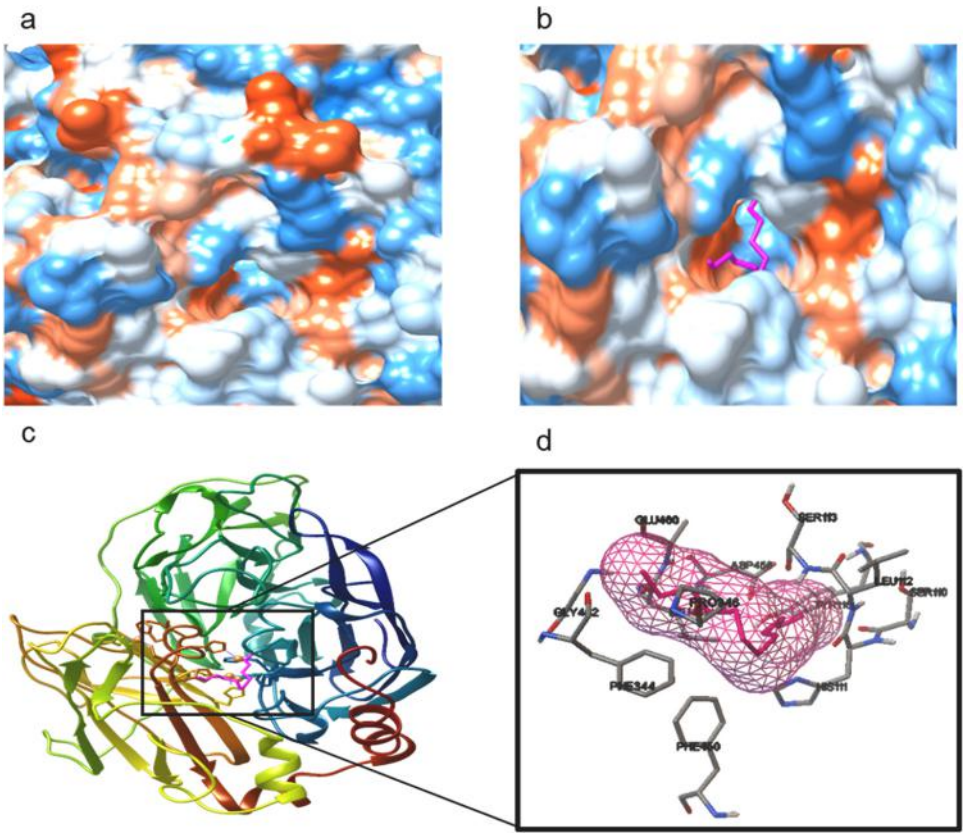

Fig. 2. *In silico* molecular docking analysis of the binding capacity of PE with Lac. Lac cavity (a), representation of the PE-Lac complex hydrophobic surface, PE on magenta (software UCSF Chimera) (b), docked PE-Lac structure, PE on magenta and Lac depicted on secondary structure with rainbow colors from n-terminus in blue to c-terminus in red (software UCSF Chimera) (c), and binding site showing PE in magenta and surrounding amino acid residues on colors by heteroatom (software AutoDockTools) (d).(For interpretation of the references to colour in this figure legend, the reader is referred to the web version of this article.)

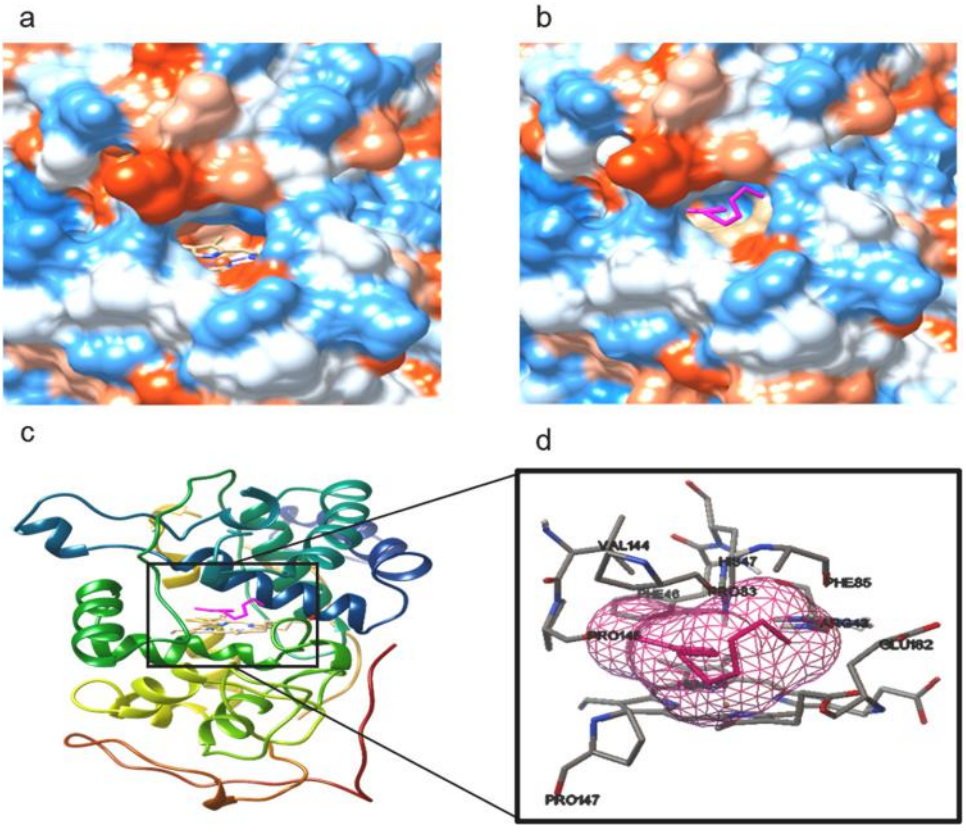

Fig. 3. *In silico* molecular docking analysis of the binding capacity of PE with LiP. LiP cavity (a), representation of the PE-LiP complex hydrophobic surface, PE on magenta (software UCSF Chimera) (b), docked PE-LiP structure, PE on magenta and LiP depicted on secondary structure with rainbow colors from n-terminus in blue to c-terminus in red (software UCSF Chimera) (c), and binding site showing PE in magenta and surrounding amino acid residues on colors by heteroatom (software AutoDockTools) (d).(For interpretation of the references to colour in this figure legend, the reader is referred to the web version of this article.)

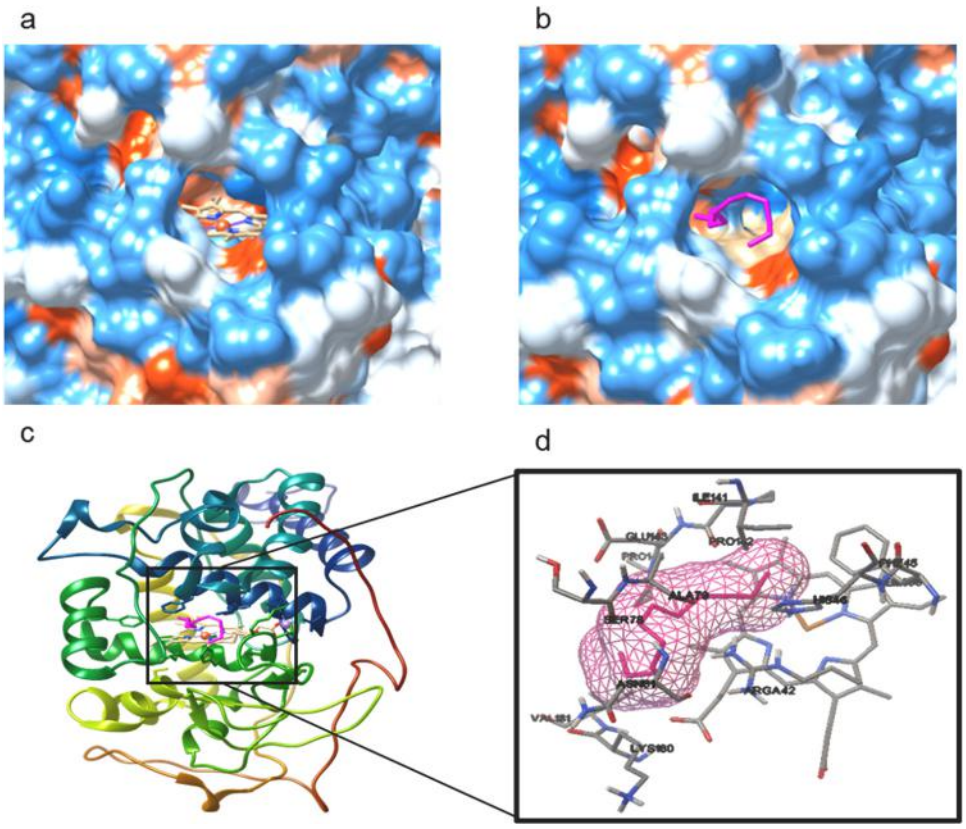

Fig. 4. *In silico* molecular docking analysis of the binding capacity of PE with MnP. MnP cavity (a), representation of the PE-MnP complex hydrophobic surface, PE on magenta (software UCSF Chimera) (b), docked PE-MnP structure, PE on magenta and MnP depicted on secondary structure with rainbow colors from n-terminus in blue to c-terminus in red (software UCSF Chimera) (c), and binding site showing PE in magenta and surrounding amino acid residues on colors by heteroatom (software AutodockTools) (d).(For interpretation of the references to colour in this figure legend, the reader is referred to the web version of this article.)

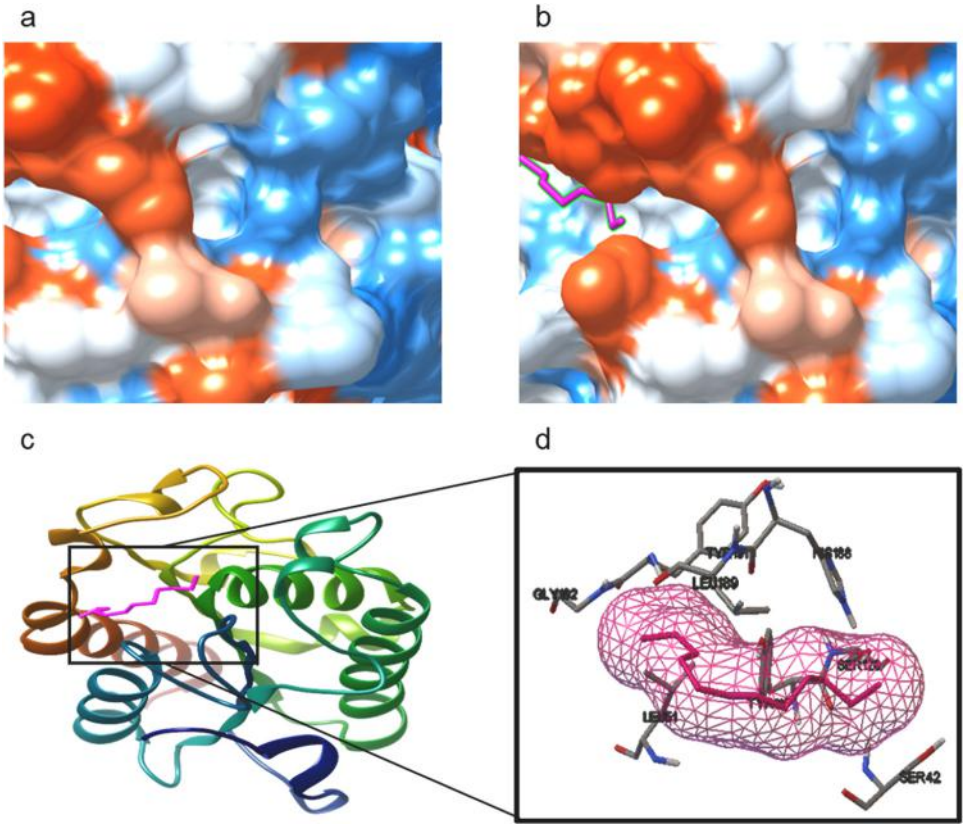

Fig. 5. *In silico* molecular docking analysis of the binding capacity of PE with Cut. Cut cavity (a), representation of the PE-Cut complex hydrophobic surface, PE on magenta (software UCSF Chimera) (b), docked PE-Cut structure, PE on magenta and enzyme depicted on secondary structure with rainbow colors from n-terminus in blue to c-terminus in red (software UCSF Chimera) (c), and binding site showing PE in magenta and surrounding amino acid residues on colors by heteroatom (software AutodockTools) (d).(For interpretation of the references to colour in this figure legend, the reader is referred to the web version of this article.)

Table 2
PE-binding energy, PE-binding affinity and dimensions of the PE-binding-site in the cavity of the enzyme estimated by molecular docking calculations.

Enzyme	E.C.	PE-binding energy (Kcal/mol)	PE-binding affinity (μM)	PE-binding-site cavity area (Å^2)	volume (Å^3)
UnP	1.11.2.1	-6.09	34.34	659.920	367.243
Lac	1.10.3.2	-6.00	40.11	217.333	153.052
LiP	1.11.1	-5.69	66.93	604.068	343.361
MnP	1.11.1.13	-5.57	82.16	552.080	273.023
Cut	3.1.1	-3.07	5590	67.935	29.114

and a volume between 401.72 and 2106.88 Å^3 (do Canto et al., 2019). The diverse sizes of area and volume of binding sites are important features in enzyme substrate selectivity.

3.2. Enzyme-catalyzed PE degradation hypothetical pathways proposal

A previous study found that Lac, MnP, and LiP were produced extracellularly by several fungal isolates that were capable of breaking down and consuming PE (Ameen et al., 2015). These enzymes catalyze several reactions to degrade their substrates. Laccases transfer electrons from organic substrates to molecular oxygen, whereas MnP and LiP (heme peroxidases) undergo oxidation-reduction reactions using H_2O_2 as an electron accepting cosubstrate (Sánchez, 2020). In particular, UnP from the fungi *Marasmius rotula* and *Agrocybe aegerita* has been reported to be capable of degrading the majority of compounds listed as US EPA (Environmental Protection Agency) priority pollutants. These enzymes are hybrids of heme peroxidases and P450 monooxygenases and catalyze several reactions (e.g., hydroxylation, epoxidation, desulfuration, dealkylation, sulfoxidation, n-oxide reduction, dehalogenation and deamination) (Karich et al., 2017; Shin et al. 2018).

In this work, five hypothetical pathways were proposed for the enzymatic degradation of PE under aerobic conditions. Four proposals are shown using MnP, Lac, LiP or UnP as individual enzymes, and a pathway is proposed using a synergic enzymatic combination of Lac, LiP and MnP. In all cases, the degradation pathway was proposed using (hypothetically) a fungal hydrophobin from class II (Wu et al. 2017), which acts as a biosurfactant so enzymatic catalysis can be carried out.

Fig. 6 shows a hypothetical PE degradation pathway by MnP from *P. chrysosporium* (Sundaramoorthy et al., 2010). This pathway was proposed on the basis of previously detected intermediate compounds (Balasubramanian et al. 2014, Sánchez, 2020). The catalytic active site of MnP includes aspartate (Asp179), alanine (Ala79), serine (Ser78), arginine (Arg42), glutamate (Glu35, Glu143, Glu39), asparagine (Asn81), histidine (His46), phenylalanine (Phe45), proline (Pro142), heme propionate, and two water molecules (a). MnP would require acidic conditions and H_2O_2 (which should be added to the culture medium) to begin its catalytic activity·H_2O_2 is an oxidizing agent that splits into two OH free radicals by homolytic cleavage. After H_2O_2 is broken, one OH free radical would bind to the hydrogen water of the heme MnP, and the other would bind to Fe^{2+}, liberating a H_2O molecule (b). As a consequence, the iron-porphyrin complex would be homolytically cleaved, generating porphyrin π-cation free radicals and hydroxyferryl center free radicals. Porphyrin π-cation free radicals bind the hydrogen of the hydroxyferryl center free radical, and the oxygen of propionate binds covalently to the hydrogen water, generating oxymanganese free radicals (c). PE enters the active site of MnP and reacts with oxygen of the oxymanganese free radical to form the oxoferryl-MnP free radical complex (d). As a result, PE breaks down into several small molecules, such as alkanes (e.g., dodecane and nonadecane), alkane free radicals (e.g., dodecane free radicals), ethyl free radicals and ethanol (e). Ethanol would be subsequently oxidized to acetic acid (f), which would enter the Krebs cycle (g).

On the other hand, some molecules generated by PE breakdown (e.g., alkanes, alkane free radicals and ethyl free radicals) could enter the catalytic site of MnP and break down, generating an oxymanganese free radical, which would cause a subsequent oxidation reaction (h). Alternatively, alkane free radicals (e.g., dodecane free radicals and other alkane free radicals) would be successively oxidized to dodecanal (i), which would be oxidized to dodecanoic acid (j). Dodecanoic acid reacts with ethyl free radicals to produce tetradecanoic acid (k). Tetradecanoic acid reacts with CoA to form tetradecanoyl-CoA (l) (which breaks down into fatty acids). Tetradecanoyl-CoA undergoes β-oxidation to produce acetyl CoA (m), which enters the Krebs cycle to be mineralized to CO_2 and H_2O (n) (White and Rusell, 1994). The substrate-free MnP would have an empty substrate-binding site (o) and would react with another PE molecule to restart a new catalytic cycle (p) (Sánchez, 2020).

Fig. 7 shows a hypothetical PE degradation pathway by Lac from *T. versicolor* (Bertrand et al., 2002). The catalytic site of Lac contains four copper ions, which are organized in three Cu centers (Cu_1, Cu_2 and Cu_3). Cu_1 is bound to two histidines (His395 and His458), a cysteine (Cys453) and a 2,5-dimethyl-aniline (Xyd514), forming a mononuclear center that participates in organic substrate oxidation. Cu_1 is coordinated to a trinuclear cluster formed by Cu_2 and a pair of Cu_3 (a)·H_2O_2 would be produced as a result of the reoxidation of FAD with molecular oxygen, forming an oxy trinuclear copper cluster free radical (b). PE comes into contact with the active site of Lac and reacts with Cu_1, releasing an electron, which binds the hydroxyl group of the Cu_2 center, liberating a water molecule (c). The three Cu centers would produce an electron flux, which would regulate the presence of H_2O_2 in the medium·H_2O_2 would be broken down in two OH free radicals, one of which would bind the pair of Cu_3, generating PE free radicals, whereas the other OH free radical releases a water molecule. PE free radicals would be homolytically cleaved, forming alkane free radicals (e.g., ethyl free radicals) (d). Lac has high redox potential, which causes subsequent oxidation of its near-neighboring molecules. Therefore, alkane free radicals would be oxidized to alcohols (e.g., ethanol), releasing a water molecule (e). Alcohols would be subsequently oxidized to aldehydes (e.g., ethanal) (f) and then to carboxylic acids (e.g., acetic acid), which would enter the Krebs cycle to be mineralized to CO_2 and H_2O (g). A substrate-free Lac would react with another PE molecule to initiate a new catalytic cycle (h).

A hypothetical PE degradation pathway by LiP from *T. cervine* (Miki et al., 2011) is shown in Fig. 8. The catalytic active site of LiP includes an iron-porphyrin center, arginine (Arg43), phenylalanine (Phe46, Phe85), histidine (His47), proline (Pro83, Pro146, Pro147), valine (Val144), and glutamine (Glu182) (a). The iron-porphyrin complex undergoes homolytic N–Fe^{3+} bond cleavage to form the porphyrin π-cation free radical·H_2O_2 breaks down into two OH free radicals, one of which binds hydrogen from propionic acid, and the other binds Fe^{3+}, liberating a water molecule (b). Then, the oxyferry complex would be formed by Fe^{4+} oxidation, which would react with PE via the generation of free radicals, liberating a water molecule (c). As a result, alkane free radicals would be formed, which would be oxidized to alcohols (e.g., nonadecanol) in the presence of H_2O_2 and would release a water molecule (d). Alcohols would be oxidized to carboxylic acids, and as a result, they would form the heme iron-superoxo complex free radical, liberating a water molecule (e). Carboxylic acids enter the Krebs cycle to be mineralized to CO_2 and H_2O (f). The substrate-free LiP would have an empty substrate-binding site (g) and would react with a PE molecule to initiate another catalytic cycle (h).

Fig. 9 shows a hypothetical PE degradation pathway by UnP from *A. aegerita* (Piontek et al., 2013). The catalytic active site of UnP includes valine (Val244), phenylalanine (Phe121, Phe191, Phe199 and Phe274), alanine (Ala77), threonine (Thr192), glycine (Gly195), glutamate (Glu196), serine (Ser123), cysteine (Cys33), heme propionate, 1H-imidazol-5-yl methanol (Mzo354) and two water molecules that bind to manganese (a). PE degradation by UnP would require the presence of H_2O_2 in the medium·H_2O_2 would be produced as a result of the reoxidation of FAD with molecular oxygen. In this case, cysteine acts as an acid/base catalyst, donating its electrons so that Fe^{3+} reacts with H_2O_2

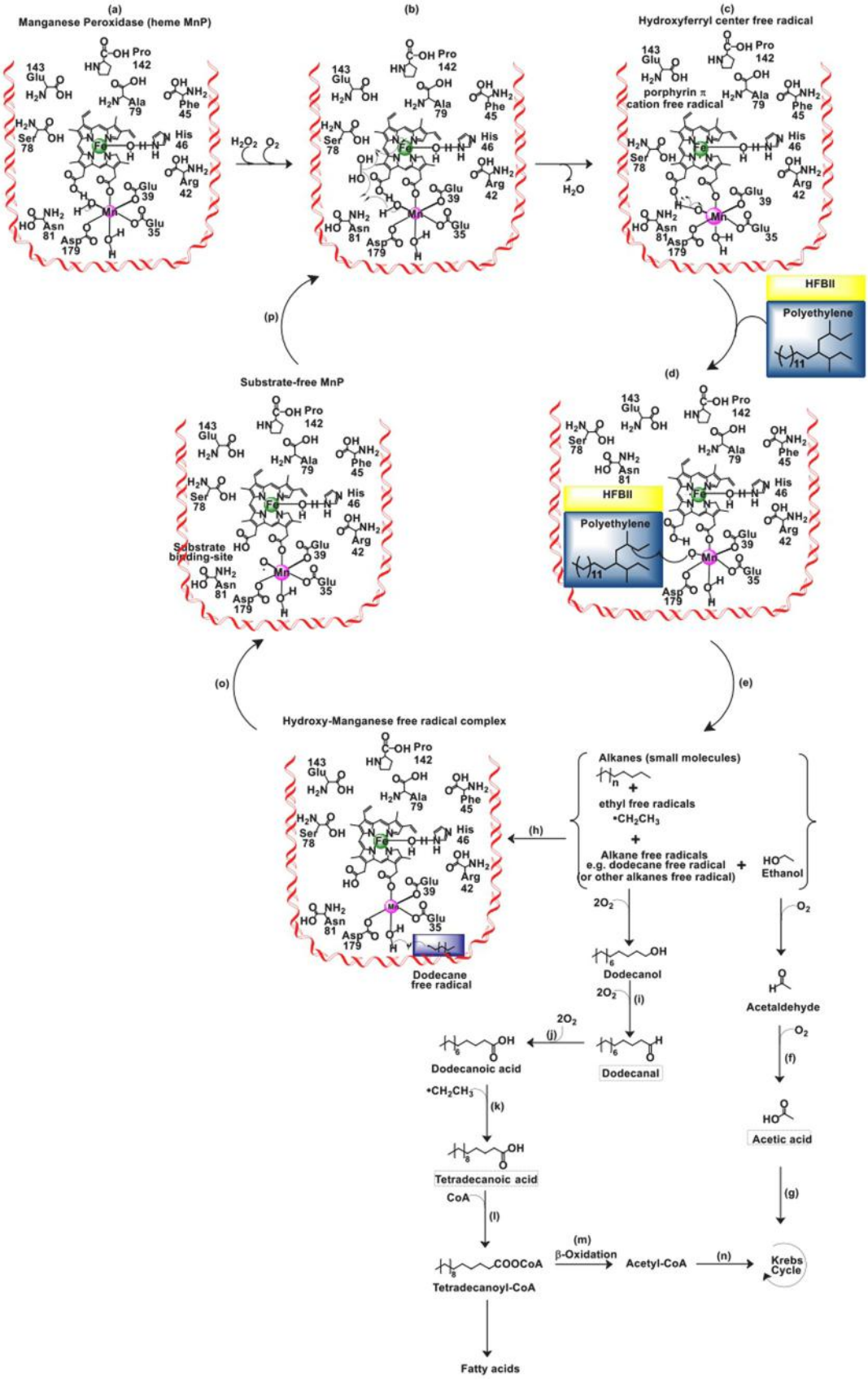

Fig. 6. Hypothetical PE degradation pathway by MnP from *P. chrysosporium*. The catalytic active site of MnP includes Asp179, Ala79, Ser78, Arg42, Glu35, Glu143, Glu39, Asn81, His46, Phe45, Pro142, heme propionate, and two water molecules. This pathway was proposed on the basis of previously detected intermediate compounds (Balasubramanian et al. 2014).
Redrawn from Sánchez (2020).

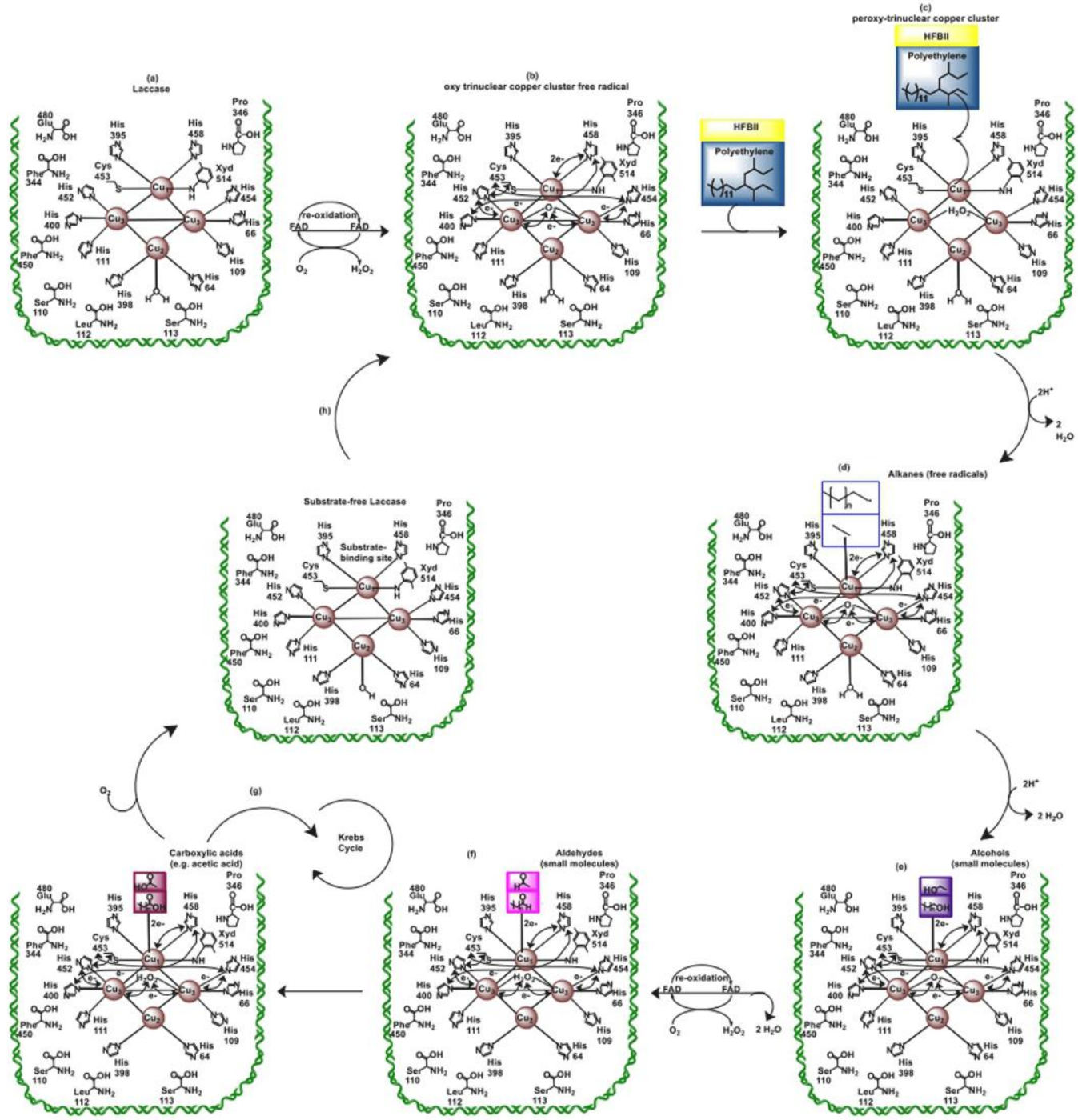

Fig. 7. Hypothetical PE degradation pathway by Lac from *T. versicolor*. The catalytic site of Lac contains four copper ions, which are organized in three Cu centers (Cu_1, Cu_2 and Cu_3). Cu_1 is bound to two histidines (His395 and His458), a cysteine (Cys453) and a 2,5-dimethyl-aniline (Xyd514).

(b). FAD reacts with hydrogen of H_2O_2 and forms a heme iron-superoxo complex, which oxidizes Fe^{4+}, forming the oxoferryl complex and liberating a water molecule (c). The oxoferryl complex reacts with PE to begin its catalysis (d), generating alkanes (small molecules), ethyl free radicals and alkane free radicals (e.g., dodecane free radicals) (e). Alkanes, alkane free radicals and ethyl free radicals are successively oxidized to acetic acid, which enters the Krebs cycle to be mineralized to CO_2 and H_2O (f). Alternatively, alkane free radicals would form acetyl-CoA by β-oxidation, which would also enter the Krebs cycle (g) (as mentioned previously for the MnP catalytic cycle). The PE-free UnP would then have an unoccupied PE-binding site (h), which would restart a new catalytic cycle (i).

On the other hand, enzymes can act synergistically for complete breakdown of their substrate (Sánchez, 2020). Ameen et al. (2015) detected Lac, MnP, and LiP activities in several fungal isolates that were capable of degrading PE. Therefore, a hypothetical PE degradation pathway using a synergic enzymatic combination of Lac, LiP and MnP is shown in Fig. 10. As an oxidase, Lac is able to produce H_2O_2 as a side-product, a substance required by peroxidases for catalytic oxidation of a substrate (i.e., PE). Therefore, PE biodegradation would start with Lac catalytic action. The catalytic site of Lac includes Cu centers and the rest of the components mentioned before (for the Lac catalytic cycle)

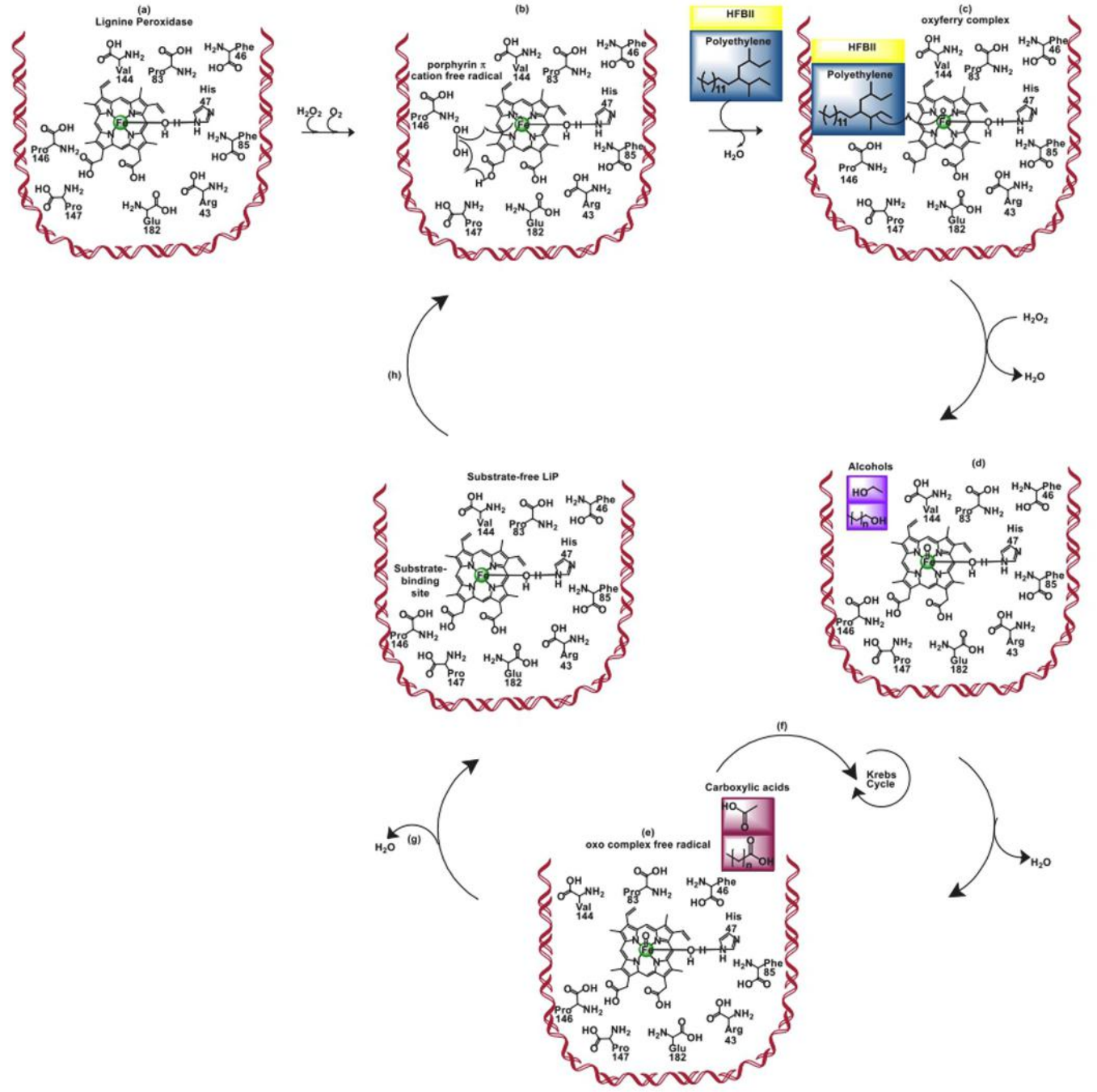

Fig. 8. Hypothetical PE degradation pathway by LiP from *T. cervine*. The catalytic active site of LiP includes an iron-porphyrin center, Arg43, Phe46, Phe85, His47, Pro83, Pro146, Pro147, Val144, and Glu182.

(Bertrant et al., 2002) (a). Cysteine (Cis453) donates its pair of electrons to Cu_1, forming an oxy-trinuclear copper cluster free radical (b). Cu_1 reacts with PE by a radical coupling mechanism. This process of partial PE degradation would form peroxy-trinuclear copper clusters and would provide H_2O_2 to LiP and MnP for PE subsequent catalysis, releasing 2 water molecules during this process (c). In the next step, the activation of LiP would start with the oxidation of the heme iron center, which would react with the PE, releasing a water molecule (d). As a result, PE-free radicals would be formed, which would react with the heme iron center (e), liberating alkanes (small molecules), ethyl free radicals and alkane free radicals (such as dodecane free radicals) and ethanol (f). MnP would carry out the final degradation step in the PE catalytic process. Those molecules generated by PE breakdown (e.g., alkanes, alkane free radicals, ethyl free radicals) would enter the MnP catalytic site where they would be broken down into organic acids (g), which would enter the Krebs cycle to be mineralized to CO_2 and H_2O (h). Alternatively, alkane free radicals and ethanol eventually enter the Krebs cycle, as previously mentioned (for the MnP catalytic cycle) (i). Then, Lac would start a new catalytic cycle in this proposed synergic enzyme combination (j).

Previously, PE degradation by several fungal isolates, both individually and by a consortium, was studied, in which MnP, Lac and LiP activities were evaluated (Ameen et al., 2015). In general, MnP showed the highest activity, followed by LiP and Lac (Ameen et al., 2015). These results are in accordance with the present study, since of these three enzymes, MnP and LiP showed a major participation in PE

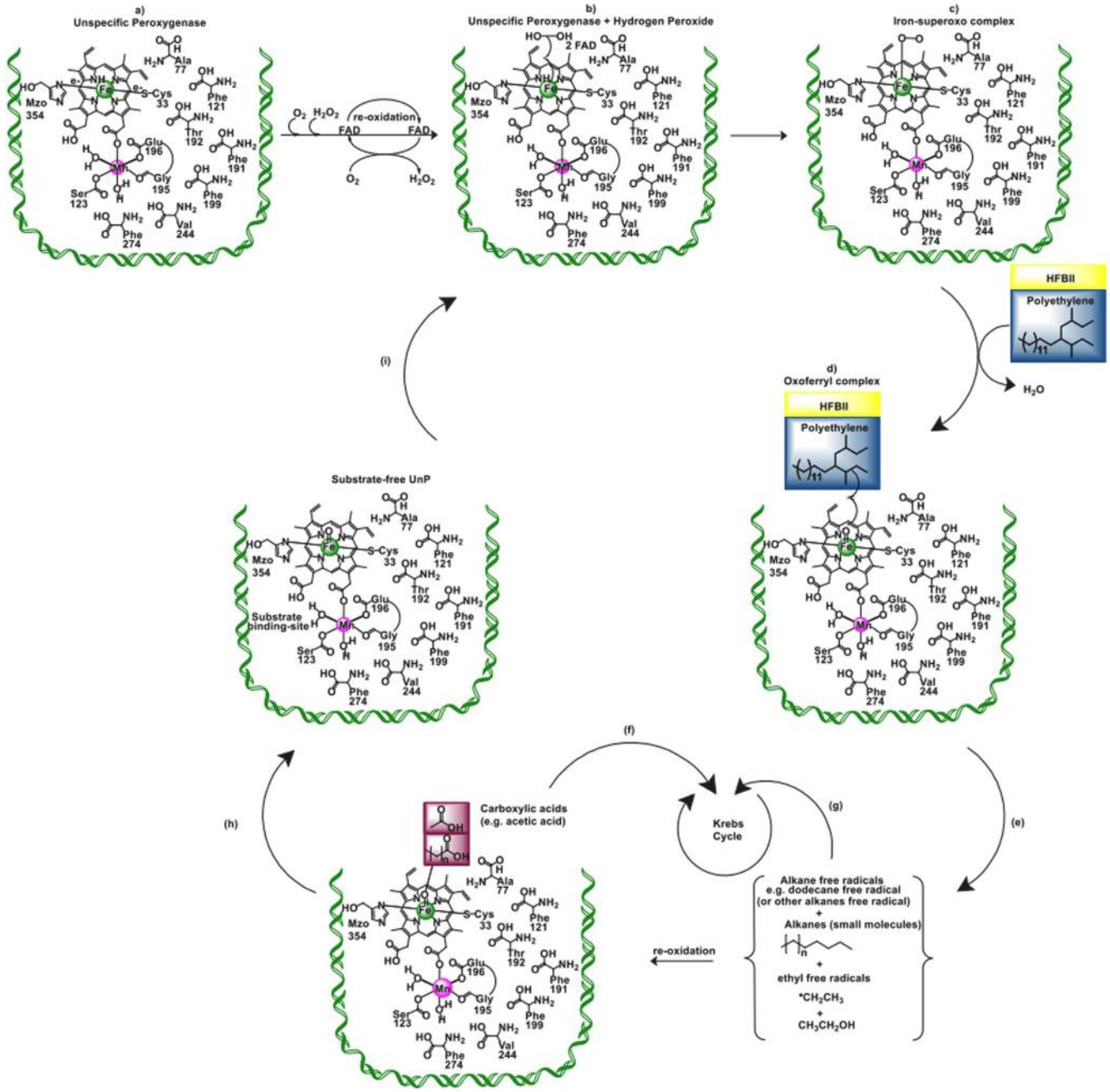

Fig. 9. Hypothetical PE degradation pathway by UnP from *A. aegerita*. The catalytic active site of UnP includes Val244, Phe121, Phe191, Phe199, Phe274, Ala77, Thr192, Gly195, Glu196, Ser123, Cys33, heme propionate, 1H-imidazol-5-yl methanol (Mzo354) and two water molecules.

biodegradation. However, Lac is required to provide H_2O_2 to MnP and LiP during the PE degradation process. The Lac cavity is small, and only a part of the PE (another part is exposed to the exterior of the enzyme) would enter into the binding site for the catalytic activity. MnP and LiP have higher cavities, which would allow a more efficient degradation process, and both enzymes would participate in the catalysis of molecules once H_2O_2 is present in the medium, as shown in Fig. 10.

4. Conclusion

These findings represent an important contribution to expand our knowledge on the mechanisms of enzyme-catalyzed reactions in the PE degradation process. These results show that in nature, enzymes act in a synergic enzymatic combination, using their specific features to undertake an extraordinarily effective sequential catalytic process for organopollutants degradation. In this process, oxidases (e.g., laccases) are crucial to provide H_2O_2 to the medium (in aerobic conditions) to ensure pollutant breakdown. UnP is a versatile enzyme that offers a promising practical application for the degradation of PE and other pollutants due to the distinctive characteristics of its cavity. Molecular docking is a very useful tool to complement experimentation to elucidate the best enzyme or enzyme combination for efficient environmental decontamination. The use of microorganisms and their enzymes represents the most ecofriendly and effective decontamination approach to clean our planet of PE and other emerging contaminants.

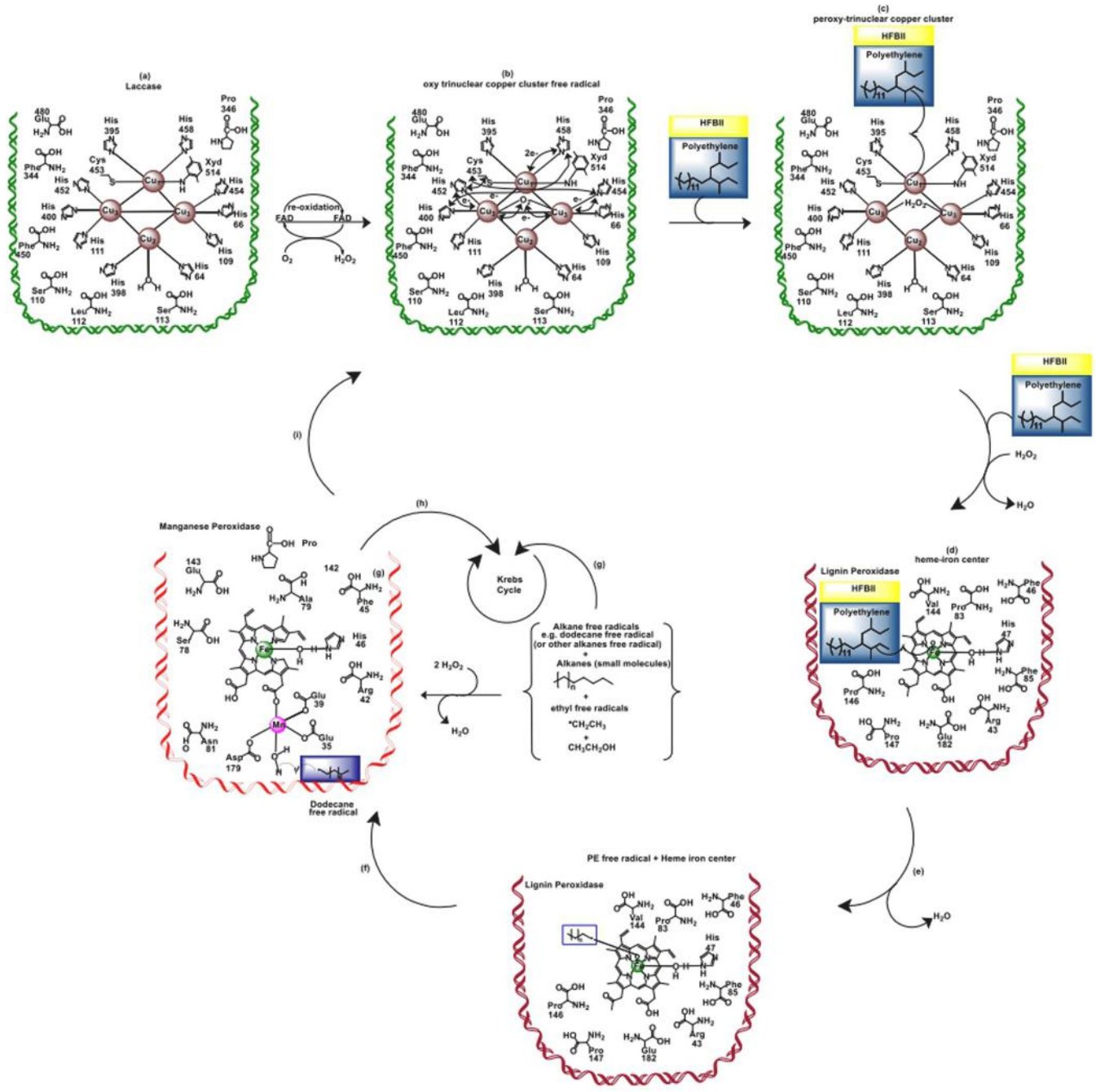

Fig. 10. Hypothetical PE degradation using a synergic enzymatic combination of Lac, LiP and MnP. Lac is able to produce H_2O_2 as a side-product, a substance required by LiP and MnP for catalytic oxidation of a substrate (i.e., PE).

CRediT authorship contribution statement

Ericka Santacruz-Juárez proposed the PE biodegradation pathways. Ricardo E. Buendia-Corona and Ramses E. Ramírez did the molecular docking analysis. Carmen Sánchez proposed the PE biodegradation pathways and wrote the MS. All authors read and approved the final manuscript.

Declaration of Competing Interest

The authors declare that they have no known competing financial interests or personal relationships that could have appeared to influence the work reported in this paper.

Acknowledgements

The work in C. Sánchez's lab has been supported by the Mexican Council for Science and Technology (CONACyT), current grant 1549 (Fronteras de la Ciencia).

REFERENCES

Aamir, M., Singh, V.K., Dubey, M.K., Meena, M., Kashyap, S.P., Katari, S.K., Upadhyay, R.S., Umamaheswari, A., Singh, S., 2018. *In silico* prediction, characterization, molecular docking, and dynamic studies on fungal SDRs as novel targets for searching potential fungicides against *Fusarium* wilt in tomato. Front. Pharmacol. 9, 1038.

Agamuthu, P., 2018. Marine debris, plastics, microplastics and nano-plastics: what next? Waste Manag. Res. 36, 869–871.

Ameen, F., Moslem, M., Hadi, S., Al-Sabri, A.E., 2015. Biodegradation of low density polyethylene (LDPE) by mangrove fungi from the Red Sea Coast. Prog. Rubber Plast. Recycl. Technol. 31, 125–144.
Awasthi, S., Srivastava, N., Singh, T., Tiwary, D., Mishra, P.K., 2017. Biodegradation of thermally treated low density polyethylene by fungus *Rhizopus oryzae* NS 5. 3 Biotech 7 (1), 73.
Balasubramanian, V., Natarajan, K., Rajeshkannan, V., Perumal, P., 2014. Enhancement of in vitro high-density polyethylene (HDPE) degradation by physical, chemical and biological treatments. Environ. Sci. Pollut. Res. Int. 21, 12549–12562.
Bertrand, T., Jolivalt, C., Briozzo, P., Caminade, E., Joly, N., Madzak, C., Mougin, C., 2002. Crystal structure of a four-copper laccase complexed with an arylamine: Insights into substrate recognition and correlation with kinetics. Biochemistry 41 (23), 7325–7333.
do Canto, V.P., Thompson, C.E., Netz, P.A., 2019. Polyurethanases: three-dimensional structures and molecular dynamics simulations of enzymes that degrade polyurethane. J. Mol. Graph. Model. 89, 82–95.
Chaudhary, A.K., Vijayakumar, R.P., 2020. Effect of chemical treatment on biological degradation of high-density polyethylene (HDPE). Environ. Dev. Sustain. 22, 1093–1104.
Das, M.P., Kumar, S., 2014. Microbial deterioration of low density polyethylene by *Aspergillus* and *Fusarium* sp. Int. J. ChemTech Res. 6, 299–305.
Deepika, S., Jaya, M.R., 2015. Biodegradation of low density polyethylene by micro-organisms from garbage soil. J. Exp. Biol. Agric. Sci. 3, 15–21.
Demain, A.L., Sánchez, S., 2017. Enzymes of industrial interest. Mex. J. Biotechnol. 2 (2), 74–97.
Esmaeili, A., Pourbabaee, A.A., Alikhani, H.A., Shabani, F., Esmaeili, E., 2013. Biodegradation of low-density polyethylene (LDPE) by mixed culture of *Lysinibacillus xylanilyticus* and *Aspergillus niger* in soil. PLoS One 8, e71720.
Fecker, T., Galaz-Davison, P., Engelberger, F., Narui, Y., Sotomayor, M., Parra, L.P., Ramírez-Sarmiento, C.A., 2018. active site flexibility as a hallmark for efficient PET degradation by *I. sakaiensis* PETase. Biophys. J. 114 (6), 1302–1312.
Frisch, M.J., Trucks, G.W., Schlegel, H.B., Scuseria, G.E., Robb, M.A., Cheeseman, J.R., Scalmani, G., Barone, V., Mennucci, B., Petersson, G.A., Nakatsuji, H., Caricato, M., Li, X., Hratchian, H.P., Izmaylov, A.F., Bloino, J., Zheng, G., Sonnenberg, J.L., Hada, M., Ehara, M., Toyota, K., Fukuda, R., Hasegawa, J., Ishida, M., Nakajima, T., Honda, Y., Kitao, O., Nakai, H., Vreven, T., Montgomery Jr., J.A., Peralta, J.E., Ogliaro, F., Bearpark, M., Heyd, J.J., Brothers, E., Kudin, K.N., Staroverov, V.N., Kobayashi, R., Normand, J., Raghavachari, K., Rendell, A., Burant, J.C., Iyengar, S. S., Tomasi, J., Cossi, M., Rega, N., Millam, J.M., Klene, M., Knox, J.E., Cross, J.B., Bakken, V., Adamo, C., Jaramillo, J., Gomperts, R., Stratmann, R.E., Yazyev, O., Austin, A.J., Cammi, R., Pomelli, C., Ochterski, J.W., Martin, R.L., Morokuma, K., Zakrzewski, V.G., Voth, G.A., Salvador, P., Dannenberg, J.J., Dapprich, S., Daniels, A.D., Farkas, O., Foresman, J.B., Ortiz, J.V., Cioslowski, J., Fox, D.J., 2010. Gaussian 09, Revision B.01. Gaussian Inc., Wallingford. CT, USA.
Gasteiger, J., Marsili, M., 1980. Iterative partial equalization of orbital electronegativity-a rapid access to atomic charges. Tetrahedron 36 (22), 3219–3228.
Helmberger, M.S., Tiemann, L.K., Grieshop, M.J., 2020. Towards an ecology of soil microplastics. Funct. Ecol. 34, 550–560.
Hernández-Sánchez, B., Díaz-Godínez, R., Luna-Sánchez, S., Sánchez, C., 2019. Esterase production by microorganisms: importance and industrial application. Mex. J. Biotechnol. 4 (1), 25–37.
Isvoran, A., 2015. Web-based computational tools used in protein surface analysis and characterization. Applications for protein–protein and protein–ligand interactions. In: Putz, M., Ori, O. (Eds.), Exotic Properties of Carbon Nanomatter, Carbon Materials: Chemistry and Physics, vol. 8. Springer, Dordrecht.
Ju, H., Zhu, D., Qiao, M., 2019. Effects of polyethylene microplastics on the gut microbial community, reproduction and avoidance behaviors of the soil springtail, Folsomia candida. Environ. Pollut. 247, 890–897.
Karich, A., Ullrich, R., Scheibner, K., Hofrichter, M., 2017. Fungal unspecific peroxygenases oxidize the majority of organic EPA priority pollutants. Front. Microbiol. 8, 1463.
Kastritis, P.L., Bonvin, A.M.J.J., 2013. On the binding affinity of macromolecular interactions: daring to ask why proteins interact. J. R. Soc. Interface 10, 20120835.
Kurtz, S., Manley, M., 2009. Cross-linked polyethylene. In: Hozack, W., Parvizi, J., Bender, B. (Eds.), Surgical Treatment of Hip Arthritis. Reconstruction, Replacement, and Revision. Saunders (W.B.) Co Ltd, pp. 456–467.
Li, X., Chu, Z., Du, X., Qiu, Y., Li, Y., 2019. Combined molecular docking, homology modelling and density functional theory studies to modify dioxygenase to efficiently degrade aromatic hydrocarbons. RSC Adv. 9 (20), 11465–11475.
Librando, V., Pappalardo, M., 2013. *In silico* bioremediation of polycyclic aromatic hydrocarbon: a frontier in environmental chemistry. J. Mol. Graph. Model. 44, 1–8.
Liu, Z., Liu, Y., Zeng, G., Shao, B., Chen, M., Li, Z., Jiang, Y., Liu, Y., Zhang, Y., Zhong, H., 2018a. Application of molecular docking for the degradation of organic pollutants in the environmental remediation: a review. Chemosphere 203, 139–150.
Liu, Z., Shao, B., Zeng, G., Chen, M., Li, Z., Liu, Y., Jiang, Y., Zhong, H., Liu, Y., Yan, M., 2018b. Effects of rhamnolipids on the removal of 2,4,2,4-tetrabrominated biphenyl ether (BDE-47) by *Phanerochaete chrysosporium* analyzed with a combined approach of experiments and molecular docking. Chemosphere 210, 922–930.
Martinez, C., De Geus, P., Lauwereys, M., Matthyssens, G., Cambillau, C., 1992. *Fusarium solani* cutinase is a lipolytic enzyme with a catalytic serine accessible to solvent. Nature 356 (6370), 615–618.
Miki, Y., Calviño, F.R., Pogni, R., Giansanti, S., Ruiz-Dueñas, F.J., Martínez, M.J., Basosi, R., Romero, A., Martínez, A.T., 2011. Crystallographic, kinetic, and spectroscopic study of the first ligninolytic peroxidase presenting a catalytic tyrosine. J. Biol. Chem. 286 (17), 15525–15534.
Mishra, S., Wang, W., de Oliveira, I.P., Atapattu, A.J., Xia, S.W., Grillo, R., Honaiser-Lescano, C., Yang, X., 2021. Interaction mechanism of plant-based nanoarchitectured materials with digestive enzymes of termites as target for pest control: evidence from molecular docking simulation and in vitro studies. J. Hazard. Mater. 403, 123840.
Morris, G., Goodsell, D., Halliday, R., Huey, R., Hart, W., Belew, R., Olson, A., 1998. Automated docking using a Lamarckian genetic algorithm and an empirical binding free energy function. J. Comput. Chem. 19, 1639–1662.
Morris, G.M., Huey, R., Lindstrom, W., Sanner, M.F., Belew, R.K., Goodsell, D.S., Olson, A.J., 2009. AutoDock4 and AutoDockTools4: automated docking with selective receptor flexibility. J. Comput. Chem. 30 (16), 2785–2791.
Muhonja, C.N., Makonde, H., Magoma, G., Imbuga, M., 2018. Biodegradability of polyethylene by bacteria and fungi from Dandora dumpsite Nairobi-Kenya. PLoS One 13, e0198446.
Munir, E. , Harefa, R.S.M. , Priyani, N. , Suryanto, D. , Plastic degrading fungi Trichoderma viride and Aspergillus nomius isolated from local landfill soil in Medan. IOP Conference Series: Earth and Environmental Science 126 2018 012145.
Ojha, N., Pradhan, N., Singh, S., Barla, A., Shrivastava, A., Khatua, P., Rain, V., Bose, S., 2017. Evaluation of HDPE and LDPE degradation by fungus, implemented by statistical optimization. Sci. Rep. 7, 39515.
Paço, A., Duarte, K., da Costa, J.P., Santos, P.S.M., Pereira, R., Pereira, M.E., Freitas, A.C., Duarte, A.C., Rocha-Santos, T.A.P., 2017. Biodegradation of polyethylene microplastics by the marine fungus *Zalerion maritimum*. Sci. Total. Environ. 586, 10–15.
Pathak, V.M., Navneet, 2017. Review on the current status of polymer degradation: a microbial approach. Bioresour. Bioprocess. 4, 15.
Pettersen, E.F., Goddard, T.D., Huang, C.C., Couch, G.S., Greenblatt, D.M., Meng, E.C., Ferrin, T.E., 2004. UCSF Chimera? a visualization system for exploratory research and analysis. J. Comput. Chem. 25 (13), 1605–1612.
Piontek, K., Strittmatter, E., Ullrich, R., Gröbe, G., Pecyna, M.J., Kluge, M., Scheibner, K., Hofrichter, M., Plattner, D.A., 2013. Structural basis of substrate conversion in a new aromatic peroxygenase. J. Biol. Chem. 288 (48), 34767–34776.
Quero, G.M., Luna, G.M., 2017. Surfing and dining on the "plastisphere": microbial life on plastic marine debris. Adv. Oceanogr. Limnol. 8, 199–207.
Raghavendra, V.B., Uzma, M., Govindappa, M., Vasantha, R.A., Lokesh, S., 2016. Screening and identification of polyurethane (PU) and low density polyethylene (LDPE) degrading soil fungi isolated from municipal solid waste. Int. J. Curr. Res. 8, 34753–34761.
Restrepo-Flórez, J.M., Bassi, A., Thompson, M.R., 2014. Microbial degradation and deterioration of polyethylene-a review. Int. Biodeterior. Biodegrad. 88, 83–90.
Sakhalkar, S., Mishra, R.L., 2013. Screening and identification of soil fungi with potential of plastic degrading ability. Indian J. Appl. Res. 3, 62–64.
Sánchez, C., 2020. Fungal potential for the degradation of petroleum-based polymers: an overview of macro- and microplastics biodegradation. Biotechnol. Adv. 40, 107501.
Sangale, M.K., Shahnawaz, M., Ade, A.B., 2019. Potential of fungi isolated from the dumping sites mangrove rhizosphere soil to degrade polythene. Sci. Rep. 9, 5390.
Selonen, S., Dolar, A., Jemec Kokalj, A., Skalar, T., Parramon Dolcet, L., Hurley, R., van Gestel, C.A.M., 2020. Exploring the impacts of plastics in soil – the effects of polyester textile fibers on soil invertebrates. Sci. Total Environ. 700, 134451.
Shao, B., Liu, Z., Zeng, G., Liu, Y., Yang, X., Zhou, C., Chen, M., Liu, Y., Jiang, Y., Yan, M., 2019. Immobilization of laccase on hollow mesoporous carbon nanospheres: noteworthy immobilization, excellent stability and efficacious for antibiotic contaminants removal. J. Hazard. Mater. 362, 318–326.
Shin, J., Kim, J.E., Lee, Y.W., Son, H., 2018. Fungal Cytochrome P450s and the P450 complement (CYPome) of *Fusarium graminearum*. Toxins 10, 112.
Sindujaa, P., Padmapriya, M., Pramila, R., Vijaya Ramesh, K., 2011. Bio-Degradation of low density polyethylene (LDPE) by fungi isolated from marine water. Res. J. Biol. Sci. 6, 141–145.
Singh, J., Gupta, K.C., 2014. Screening and identification of low density polyethylene (LDPE) degrading soil fungi isolated from polythene polluted sites around Gwalior city (M.P.). Int. J. Curr. Microbiol. Appl. Sci. 3, 443–448.
Singh, N., Dalal, V., Mahto, J.K., Kumar, P., 2017. Biodegradation of phthalic acid esters (PAEs) and *in silico* structural characterization of mono-2-ethylhexyl phthalate (MEHP) hydrolase on the basis of close structural homolog. J. Hazard. Mater. 338, 11–22.
de Souza-Machado, A.A., Kloas, W., Zarfl, C., Hempel, S., Rillig, M.C., 2018. Microplastics as an emerging threat to terrestrial ecosystems. Glob. Change Biol. 24, 1405–1416.
Sowmya, H.V., Ramalingappa, Krishnappa, M., Thippeswamy, B., 2014. Degradation of polyethylene by *Trichoderma harzianum*—SEM, FTIR, and NMR analyses. Environ. Monit. Assess. 186 (10), 6577–6586.
Sridhar, S., Chandra, J.H., 2014. Involvement of computational tools towards *in silico* remediation - synthetic textile dyes interacting with azoreductase. Int. J. ChemTech Res. 6 (9), 4412–4416.
Srinivasan, S., Sadasivam, S.K., 2018. Exploring docking and aerobic-microaerophilic biodegradation of textile azo dye by bacterial systems. J. Water Process. Eng. 22, 180–191.
Srinivasan, S., Sadasivam, S.K., Gunalan, S., Shanmugam, G., Kothandan, G., 2019. Application of docking and active site analysis for enzyme linked biodegradation of textile dyes. Environ. Pollut. 248, 599–608.
Sundaramoorthy, M., Gold, M.H., Poulos, T.L., 2010. Ultrahigh (0.93Å) resolution structure of manganese peroxidase from *Phanerochaete chrysosporium*: Implications for the catalytic mechanism. J. Inorg. Biochem. 104 (6), 683–690.
Talebian, E., Talebian, M., 2014. A comparative DFT study on the differences between normal modes of polyethylene and polyethylene glycol via B3LYP Hamiltonian and the Hartree–Fock method in multiple bases. Optik 125 (1), 228–231.

Teng, Y., Liu, R., Li, C., Xia, Q., Zhang, P., 2011. The interaction between 4-aminoantipyrine and bovine serum albumin: multiple spectroscopic and molecular docking investigations. J. Hazard. Mater. 190 (1–3), 574–581.
Tian, W., Chen, C., Lei, X., Zhao, J., Liang, J., 2018. CASTp 3.0: computed atlas of surface topography of proteins. Nucleic Acids Res. 46 (W1), W363–W367.
Veber, D.F., Johnson, S.R., Cheng, H.Y., Smith, B.R., Ward, K.W., Kopple, K.D., 2002. Molecular properties that influence the oral bioavailability of drug candidates. J. Med. Chem. 45 (12), 2615–2623.
Volkamer, A., Griewel, A., Grombacher, T., Rarey, M., 2010. Analyzing the topology of active sites: on the prediction of pockets and subpockets. J. Chem. Inf. Model. 50 (11), 2041–2052.
Volkamer, A., Kuhn, D., Grombacher, T., Rippmann, F., Rarey, M., 2012. Combining global and local measures for structure-based druggability predictions. J. Chem. Inf. Model. 52 (2), 360–372.
Wang, P., Linares-Pastén, J., Zhang, B., 2020. Synthesis, molecular docking simulation and enzymatic degradation of AB-type indole-based polyesters with improved thermal properties. Biomacromolecules 21 (3), 1078–1090.
White, G.F., Russell, N.J., 1994. Biodegradation of anionic surfactants and related molecules. In: Ratledge, C. (Ed.), Biochemistry of Microbial Degradation. Springer, Dordrecht, pp. 143–177.
Wu, Y., Li, J., Yang, H., Shin, H.J., 2017. Fungal and mushroom hydrophobins: a review. J. Mushrooms 15, 1–7.
Yadav, S., Pandey, S.K., Singh, V.K., Goel, Y., Kumar, A., Singh, S.M., 2017. Molecular docking studies of 3-bromopyruvate and its derivatives to metabolic regulatory enzymes: Implication in designing of novel anticancer therapeutic strategies. PLoS One 12, e0176403.
Zago, E., Dubreucq, E., Lecomte, J., Villeneuve, P., Fine, F., Fulcrand, H., Aouf, C., 2016. Synthesis of bio-based epoxy monomers from natural allyl- and vinyl phenols and the estimation of their affinity to the estrogen receptor α by molecular docking. New J. Chem. 40 (9), 7701–7710.
Zahra, S., Abbas, S.S., Mahsa, M.T., Mohsen, N., 2010. Biodegradation of low-density polyethylene (LDPE) by isolated fungi in solid waste medium. Waste Manag. 30, 396–401.
Zhang, J., Gao, D., Li, Q., Zhao, Y., Li, L., Lin, H., Bi, Q., Zhao, Y., 2020. Biodegradation of polyethylene microplastic particles by the fungus *Aspergillus flavus* from the guts of wax moth *Galleria mellonella*. Sci. Total Environ. 704, 135931.
Zígolo, M.A., Irazusta, V.P., Rajal, V.B., 2020. Correlation between initial biodegradability determined by docking studies and structure of alkylbenzene sulfonates: a new tool for intelligent design of environmentally friendly anionic surfactants. Sci. Total Environ. 728, 138731.